

TimeMachine: Fine-Grained Facial Age Editing with Identity Preservation

Yilin Mi^{1,2*}, Qixin Yan^{2*}, Zheng-Peng Duan¹,
Chunle Guo¹, Hubery Yin², Hao Liu², Chen Li², Chongyi Li^{1†}

¹VCIP, CS, Nankai University ²WeChat Vision, Tencent Inc.
yilinmi@mail.nankai.edu.cn, qixinyan@tencent.com, lichongyi@nankai.edu.cn

Abstract

With the advancement of generative models, facial image editing has made significant progress. However, achieving fine-grained age editing while preserving personal identity remains a challenging task. In this paper, we propose **TimeMachine**, a novel diffusion-based framework that achieves accurate age editing while keeping identity features unchanged. To enable fine-grained age editing, we inject high-precision age information into the multi-cross attention module, which explicitly separates age-related and identity-related features. This design facilitates more accurate disentanglement of age attributes, thereby allowing precise and controllable manipulation of facial aging. Furthermore, we propose an Age Classifier Guidance (ACG) module that predicts age directly in the latent space, instead of performing denoising image reconstruction during training. By employing a lightweight module to incorporate age constraints, this design enhances age editing accuracy by modestly increasing training cost. Additionally, to address the lack of large-scale, high-quality facial age datasets, we construct a **HFFA** dataset (High-quality Fine-grained Facial-Age dataset) which contains **one million** high-resolution images labeled with identity and facial attributes. Experimental results demonstrate that TimeMachine achieves state-of-the-art performance in fine-grained age editing while preserving identity consistency.

1 Introduction

Human face serves as a powerful canvas, conveying not only identity but also other attributes such as age, emotion, and health. Recent advancements in image generation have led to significant progress in facial image analysis and editing. Among these techniques, age manipulation, covering both age progression and regression, has attracted increasing attention. It allows us to digitally alter the perceived age of individuals in images and videos, offering many practical and entertaining uses.

However, existing facial editing methods still face challenges in age manipulation, which can be attributed primarily to two aspects. On the one hand, early approaches rely on Generative Adversarial Networks (GANs) (Goodfellow et al. 2014) to synthesize faces with modified age attributes. They either inject age information as an additional condition into GANs, or explore age-related directions within the

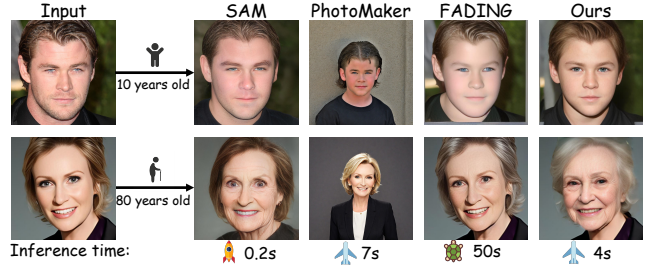


Figure 1: We compare our method with several state-of-the-art face editing approaches, including GAN-based SAM (Alaluf, Patashnik, and Cohen-Or 2021) and diffusion-based PhotoMaker (Li et al. 2024), FADING (Chen and Lathuilière 2023). Given an input image and a target age, these models generate age-edited faces while attempting to preserve identity. In comparison to these methods, our approach demonstrates significantly better identity preservation and age accuracy with shorter inference time among diffusion-based methods. Additionally, it produces highly realistic and visually high-quality results. All experiments are conducted on an NVIDIA H20 GPU. (*Zoom-in for the best view*)

latent space of pre-trained GAN models. Due to the limited generative capacity and the constrained latent space of GANs, these methods struggle to preserve facial identity and generate subtle facial nuances, which can be observed in Figure 1. Recently, diffusion models (Ho, Jain, and Abbeel 2020) have exhibited remarkable performance in generative capabilities, gradually emerging as successors to GANs in facial image editing. Despite the remarkable progress in facial image editing, they (Ye et al. 2023; Li et al. 2024; Chen and Lathuilière 2023) often treat facial attributes as an integrated whole, making it difficult to achieve targeted editing of specific features such as age. In most mature facial editing frameworks (Li et al. 2024; Wang et al. 2024; Ye et al. 2023), attributes like age, expression, and identity are deeply entangled in the latent representations, leading to unintended changes in non-target attributes during editing. Therefore, altering age might inadvertently affect facial identity or expression, resulting in artifacts or unnatural outputs. This limitation highlights the challenge of effectively decoupling age-related features from other facial attributes. To address this challenge, we propose an age editing framework based on a multi-level cross-attention control. Our ap-

*These authors contributed equally.

†Corresponding author.

proach aims to disentangle age information from other facial attributes by leveraging hierarchical feature interactions, enabling targeted and realistic age manipulation while preserving the individual’s identity and other key characteristics. This method not only enhances the precision of age editing but also sets a new direction for disentangled facial attribute manipulation in image generation.

In this paper, we address the challenge of disentangling age information from facial attributes and propose a comprehensive framework for fine-grained age editing. Our contributions include the following four aspects. **First**, by incorporating more fine-grained age information into the conditional input of the diffusion model through our proposed multi-cross attention module, we achieve enhanced feature disentanglement and precise age-aware control. This architectural innovation enables effective decoupling of age-related characteristics while maintaining accurate manipulation over age progression in the generation process. **Second**, our framework introduces implicit attribute alignment through latent-space projections of diffusion features, avoiding the conventional need for full image denoising and explicit pixel-space regression to establish age constraints. This design establishes direct age-value correspondence in feature domains, ensuring robust identity preservation and precise age manipulation compared to reconstruction-dependent methods. **Third**, to obtain purified age-specific features, we propose an innovative age-group feature averaging strategy by averaging all age embeddings within the same age cohort, in which we effectively suppress identity-related information that may be entangled in individual samples. **Fourth**, we present an HFFA dataset (High-quality Fine-grained Facial-Age dataset) addressing four critical limitations common in existing datasets: precise age annotations, high-definition image quality, rich facial detail captions, and million-scale diversity. *Together, these contributions advance the state of the art in facial age editing and provide a foundation for further exploration of disentangled attribute manipulation in image generation.*

2 Related Work

2.1 GAN-Based Facial Age Editing Methods

Early facial age editing methods (Gomez-Trenado et al. 2022; Yao et al. 2021; Alaluf, Patashnik, and Cohen-Or 2021; Or-El et al. 2020) primarily relied on Generative Adversarial Networks (GANs) (Goodfellow et al. 2014), which have shown promising capabilities in generating realistic facial images. Many of these methods work by manipulating latent vectors within the GAN’s latent space to modify age (Härkönen et al. 2020; Shen et al. 2020). However, due to the attributes in the latent space being often mixed together (Härkönen et al. 2020; Shen et al. 2020; Tov et al. 2021), these methods often result in changes to identity or other facial attributes. Furthermore, the low dimensionality and limited expressiveness of GAN latent spaces (Karras et al. 2020; Alaluf, Patashnik, and Cohen-Or 2021) constrain the ability to capture fine-grained facial details. Additionally, GAN training is unstable (Goodfellow et al. 2014; Karras et al. 2017), requiring careful tuning and often lead-

ing to mode collapse. Despite efforts (He et al. 2021; Yang et al. 2019; Hsu, Xie, and Chen 2021), most GAN-based approaches struggle with precise age control.

2.2 Diffusion Models in Face Editing

Diffusion models (Ho, Jain, and Abbeel 2020; Rombach et al. 2022; Saharia et al. 2022; Dhariwal and Nichol 2021) have recently achieved state-of-the-art results in image generation tasks, including facial synthesis and editing. These models generate images by iteratively denoising random noise, enabling the capture of complex data distributions and fine-grained facial details. Compared to GANs, diffusion models offer more stable training (Ho, Jain, and Abbeel 2020) and better preserve subtle textures such as wrinkles and facial shapes (Dhariwal and Nichol 2021; Tang et al. 2022), which are essential for age editing. However, current diffusion-based face editing methods (Couairon et al. 2022; Kavar et al. 2023) struggle with fine-grained control. Attributes like age, identity, and expression are often entangled (Liu, Li, and Sun 2019), so modifying one may unintentionally affect others. Most methods rely solely on noise prediction loss and lack explicit attribute conditioning, making precise control difficult. While some approaches add guidance during denoising (Guo et al. 2024; Liu et al. 2022), they introduce significant training overhead. Recent efforts explore more interpretable conditioning modules such as IpAdapter (Ye et al. 2023), but achieving disentangled control, especially over age, remains an open challenge, highlighting the need for more principled solutions.

3 Methodology

3.1 Preliminaries

Diffusion Model Building on Denoising Diffusion Probabilistic Models (DDPM) (Ho, Jain, and Abbeel 2020), which established foundations for iterative denoising, Stable Diffusion (SD) (Rombach et al. 2022) scales diffusion models via latent-space optimization and CLIP (Radford et al. 2021)-based text conditioning. SD maps input prompts to semantic embeddings c using CLIP’s text encoder, then learns to denoise latent representations conditioned on c by minimizing the noise prediction loss:

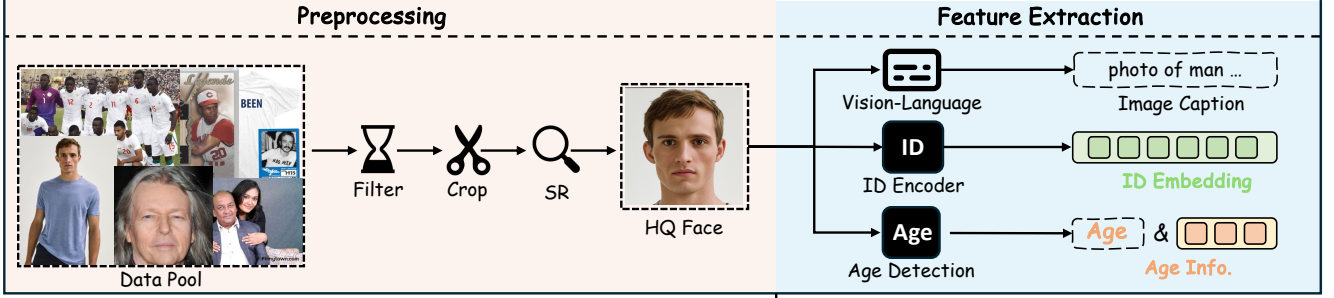
$$\mathcal{L}_{diffusion} = \mathbb{E}_{z_t, c, \epsilon, t} [\|\epsilon - \epsilon_\theta(z_t, t, c)\|_2^2], \quad (1)$$

where z_t is the noised latent code at timestep t , ϵ is the noise added to the latent z_t , and ϵ_θ is the text-conditioned denoising network.

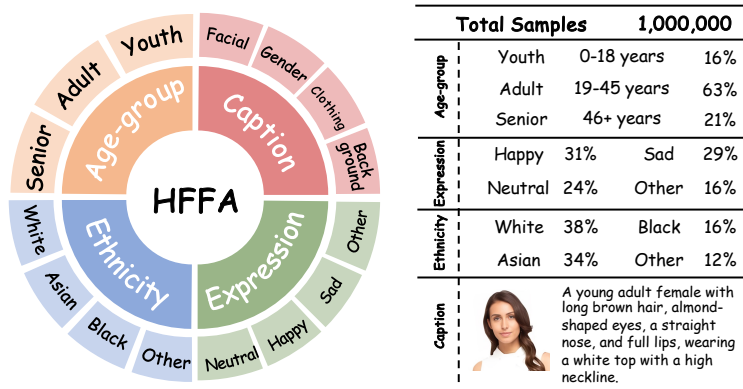
3.2 Training Data Pool Construction

High-quality training data plays a critical role in enabling fine-grained facial age editing. However, datasets with precise age labels (Matuzevičius 2024; Panis et al. 2016; Ricanek and Tesafaye 2006) tend to be limited in size, while large-scale datasets (Zheng et al. 2022) typically lack reliable annotations or contain low-resolution and noisy images. These limitations significantly hinder the training of models that require detailed age and identity information to perform fine-grained edits.

(a) Data Pipeline



(b) Face Dataset



(c) Age Codebook Construction

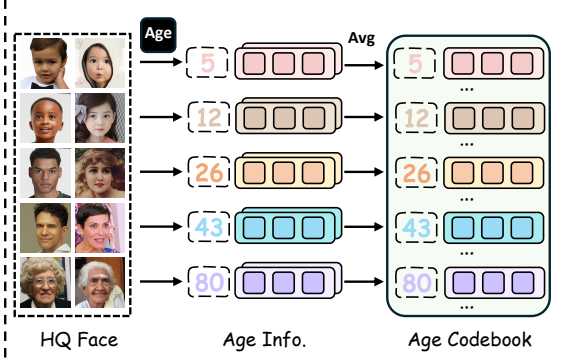


Figure 2: **HFFA** dataset construction pipeline. Each facial image in our dataset undergoes a preprocessing pipeline consisting of filtering, cropping, resizing, and super-resolution to ensure high visual quality. These refined images are passed through a pretrained age estimator, a vision-language model, and a face representation extractor to obtain rich annotations for our dataset. By averaging embeddings within the same age cohort, we create the **age codebook**, in order to extract age-specific features while minimizing identity interference.

To address this issue, as visualized in Figure 2, we construct **HFFA** dataset (High-quality Fine-grained Facial-Age dataset), which consists more than one million images, each image comes with complete annotations including a text caption (c), identity embedding (e_{id}), age embedding (e_{age}), and precise numerical age value (age). Our dataset offers two key advantages: 1) comprehensive age annotations across a wide range of age groups, and 2) high visual quality, ensuring the preservation of fine facial details essential for age transformation tasks.

To ensure the image quality of the dataset, we begin our data processing pipeline with the LAION-Face dataset (Zheng et al. 2022), supplemented by a collected private human dataset, which offers a large volume of diverse facial images.

We begin by detecting and extracting single-face regions from raw images. Each detected face is then aligned, resized, and tightly cropped to center the facial region. To further enhance the resolution and facial details, we apply CodeFormer (Zhou et al. 2022), a state-of-the-art face Super-Resolution (SR) model, to all cropped images. This ensures that even low-quality sample sources are enhanced to meet the resolution requirements of high-fidelity diffusion training. The resulting dataset contains high-quality (HQ), visually consistent single-face images suitable for precise age

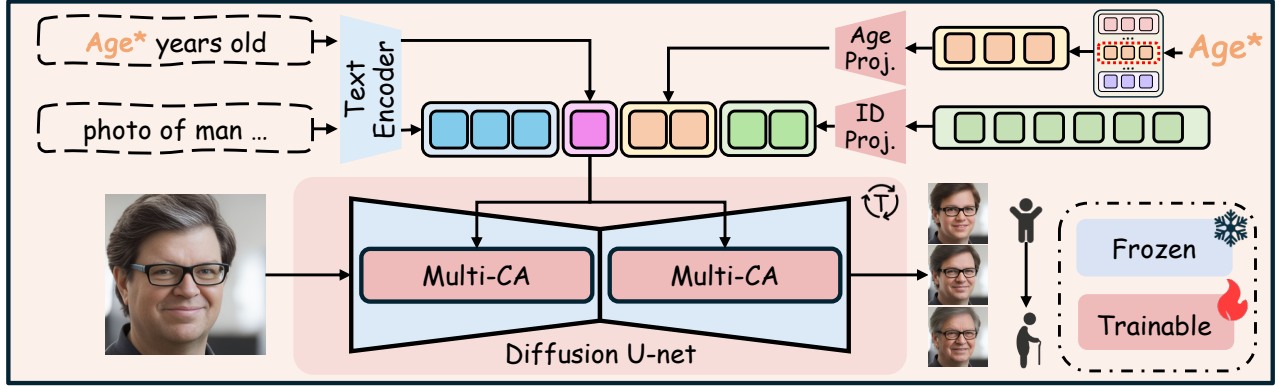
editing tasks.

For each processed image, textual descriptions are generated using the Qwen2.5VL72BInstruct (Team 2025), which provides natural language captions capturing facial attributes, context, and appearance. To obtain identity information, we utilize Antelopev2, a robust face recognition model, to extract identity embeddings e_{id} . Age information is derived using the MiVOLO model (Kuprashevich and Tolstykh 2023) in two forms: the explicit predicted numerical age from the final output layer, and the latent age embedding e_{age} from the penultimate layer. However, since the latent embedding might still mix identity information, we perform an additional step: for each age value, we average the age embeddings to compute a purified **age codebook**. This significantly reduces identity-related variance within age representations, allowing the model to better separate age-related features from identity features during training.

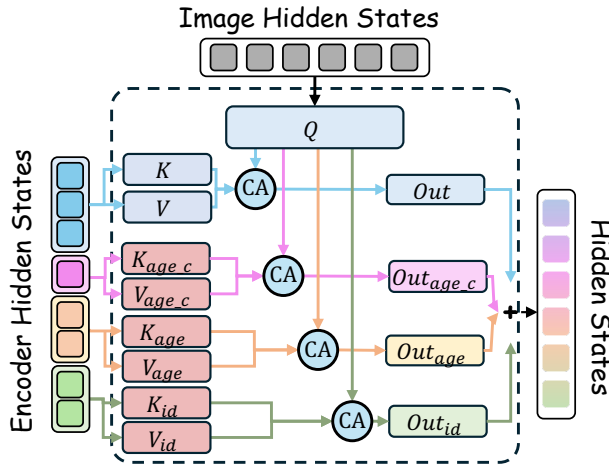
3.3 Age Editing with Multi-Attention Control

With the construction of our high-quality training data pool, we have already obtained conditioning information for each facial image, including a detailed text caption c , identity embedding e_{id} , age embedding e_{age} , and a precise numerical age label. However, an important question arises: how can we efficiently and effectively inject these conditioning sig-

(a) Pipeline



(b) Multi-Cross-Attention



(c) Training with Age Classifier Guidance

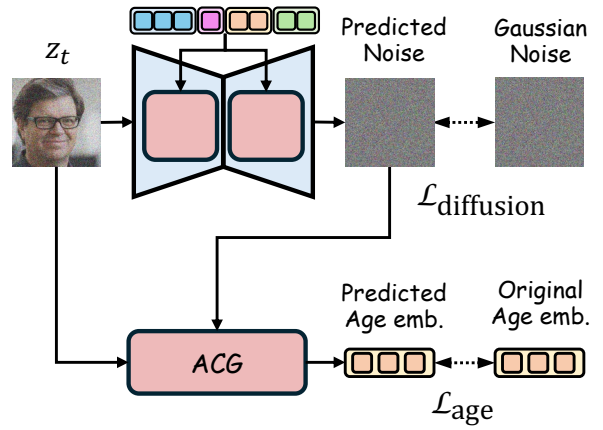


Figure 3: Overview of Fine-Grained Facial Age Editing pipeline. (a) Main Pipeline of FFAE. By combining both age and identity information as conditions, our framework guides the diffusion model to generate high-quality facial images that preserve identity while achieving precise age control. (b) The Multi-Cross Attention module disentangles combined hidden states (prompt, age, identity) into separate hidden states, each performing independent cross-attention with image features. (c) Age Classifier Guidance (ACG) module, which aligns age attributes in the latent space, enabling accurate age control without relying on pixel-level supervision.

nals into the diffusion model to guide the age editing process without compromising identity fidelity? To address this, we design a Condition Projection Module that maps identity and age embeddings into the same space as text features. These projected embeddings are then combined with caption tokens to form unified input guidance. To further enhance the editing precision, we introduce a Multi-Cross Attention mechanism within the UNet, enabling fine-grained control over age transformation and identity preservation. Detailed descriptions are provided in subsequent sections.

Condition Projection module

While prior works such as Ip-Adapter (Ye et al. 2023) utilize a projection module to inject identity features into the diffusion process, our work extends this framework by introducing an additional age projection module and enhancing the textual condition inputs to better control fine-grained age transformation. Specifically, both the identity embedding e_{id} and the age embedding e_{age} , extracted from a pre-trained

face recognition model and age estimation model respectively, are passed through separate learnable projection layers to obtain token-like representations, denoted as \hat{e}_{id} and \hat{e}_{age} . These embeddings are designed to align with the text embedding space and are concatenated with text tokens from both the image caption c and a structured age description c_{age} (e.g., 25 years old) processed through the text encoder.

In Figure 3, by enriching the textual condition with a precise age phrase and directly injecting age and identity embeddings into the condition stream, our model can better modulate the generation process across both appearance fidelity and age-specific editing. This joint conditioning setup allows the denoising UNet to better disentangle and preserve the identity information while precisely adjusting facial attributes to match the target age.

Decoupled Multi-Cross-Attention To fully use the rich condition information introduced by the Condition Projection Module, we further enhance the denoising UNet by in-

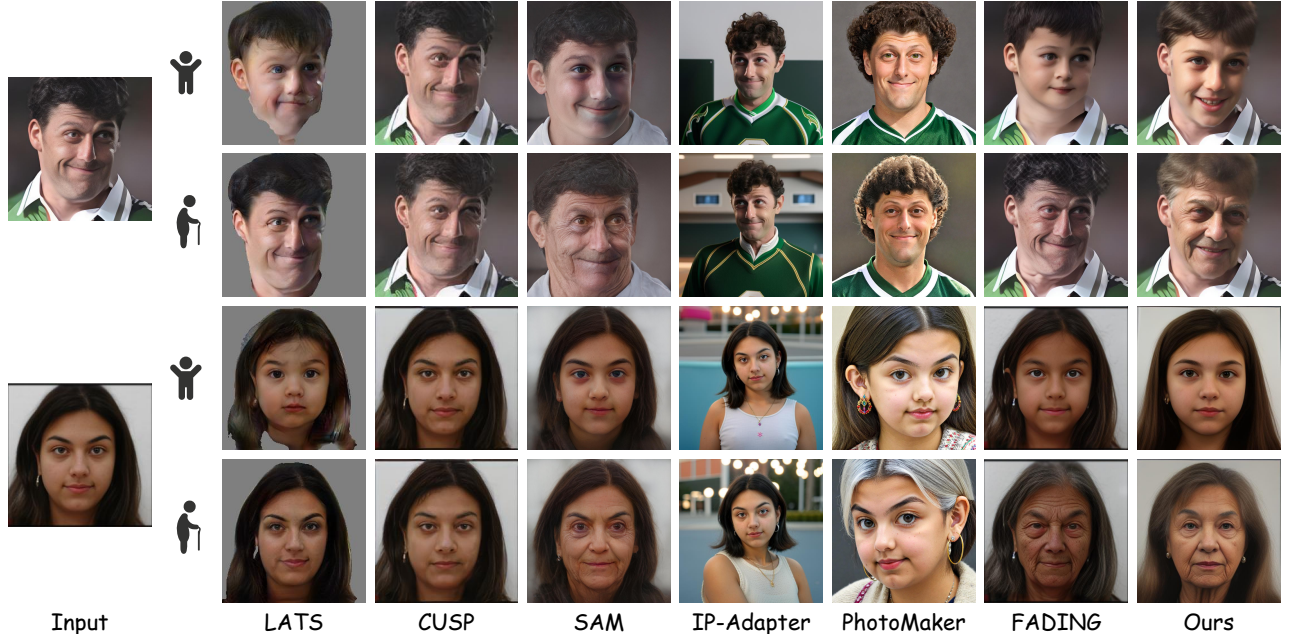


Figure 4: Qualitative comparison with state-of-the-art methods. We conduct extreme age editing generation tests on each identity, showing results at age 10 (top row) and age 80 (bottom row). Our model effectively performs age editing while preserving identity information.

tegrating a **Decoupled Multi-Cross-Attention (Multi-CA)** module within its transformer blocks. Unlike traditional single-stream cross-attention, our design enables the model to disentangle and attend to multiple semantic sources, such as identity, age, and age description separately and concurrently facilitating precise age manipulation without compromising identity.

Specifically, given the hidden features Q from the UNet and a set of condition tokens including the caption c , the structured age phrase c_{age} , and projected embeddings \hat{c}_{id} , \hat{c}_{age} , we define a set of parallel cross-attention branches. Each branch handles one condition type $i \in \{id, age, c_{age}\}$, and computes an attention output using:

$$Out_{total} = Attn(Q, K_t, V_t) + \sum_i \lambda_i \cdot Attn(Q, K_i, V_i), \quad (2)$$

where (K_t, V_t) denote the key and value derived from text caption tokens, and (K_i, V_i) are from condition-specific tokens projected into the same latent space. Each branch is modulated by a learnable or fixed scalar weight λ_i , controlling the influence of each condition stream during denoising.

This decoupled formulation enables each semantic cue to contribute independently and selectively to the generation process. The identity-related branch ensures structural consistency, while age-related streams collaboratively guide the model toward accurate age transformation.

3.4 Training with Age Classifier Guidance

Most existing face editing methods based on Stable Diffusion (SD) use a completely unsupervised training method. Specifically, they rely solely on the standard noise prediction loss $\mathcal{L}_{diffusion}$ (Eq. (1)) while modifying the architecture or adding extra modules to guide specific edits. However,

without direct supervision, these methods often struggle to precisely control target attributes, especially in fine-grained editing tasks like facial age editing.

To enhance attribute controllability, some prior works introduce additional attribute loss terms by direct denoising the latent z_t to predict x_0 , and then comparing its attributes to the target. Nevertheless, this strategy often leads to unstable training, as the one-step denoising of x_t typically yields inaccurate reconstructions of x_0 . Other methods attempt to reduce noise accumulation by using fast sampling techniques. However, these methods tend to compromise image quality or result in mode collapse when the denoising process becomes too aggressive.

To overcome these limitations, we propose an implicit constraint module, termed **Age Classifier Guidance (ACG)**. Rather than relying on fully denoised outputs, ACG leverages the noisy latent z_t , the timestep t , and the predicted noise $\epsilon_\theta(z_t, t)$ to estimate the attribute of the corresponding clean image z_0 . This provides a lightweight yet effective supervision signal for learning attribute-aware editing without disturbing the core diffusion training.

Formally, given a pre-trained age classifier $Age_{pred}(\cdot)$, the age constraint loss is defined as:

$$\mathcal{L}_{Age} = \mathbb{E}_{z_0, z_t, \epsilon, t} \left[\|Age_{pred}(z_0) - ACG(z_t, t, \epsilon)\|_2^2 \right], \quad (3)$$

where $ACG(\cdot)$ predicts the age from partially denoised latent features without requiring full image reconstruction.

To seamlessly incorporate this supervision into the diffusion training process, the total loss function is formulated as:

$$\mathcal{L}_{total} = \mathcal{L}_{diffusion} + \lambda \cdot \mathcal{L}_{Age}, \quad (4)$$

where λ is a balancing coefficient that controls the strength



Figure 5: Qualitative comparison with state-of-the-art methods. We conduct additional fine-grained age editing tests using the models that demonstrated strong performance in the extreme age editing evaluations. Our model outperforms others in terms of age editing precision, generation quality, image fidelity, realism, preservation of identity, and detail accuracy.

of the attribute constraint.

4 Experiment

4.1 Experimental Setup

Training details The model was trained based on the SD1.5 base model. The training process comprised two stages: Stage I: Initial training was conducted on our custom dataset, serving as the baseline training. Stage II: Further optimization was performed by incorporating ACG for enhanced training. Both stage utilize 8 NVIDIA H20 GPUs and a batch size of 8 per GPU.

Testing datasets For evaluation purposes, we employed the CelebA-HQ dataset (Karras et al. 2017) as our primary testing dataset. Additionally, to validate the robustness and generalizability of the models, we also tested them on the MORPH (Ricanek and Tesafaye 2006), AgeDB (Moschoglou et al. 2017), FFHQ (Karras, Laine, and Aila 2019), and CACD (Chen, Chen, and Hsu 2014) datasets. To comprehensively assess the generative performance of various age-editing models across diverse inputs, we conducted stratified random sampling across all predefined age groups, resulting in a curated subset of 100 high-resolution images with balanced age distribution. This sampling strategy ensures a statistically robust evaluation of model generalization capabilities under heterogeneous demographic conditions.

Evaluation metrics For a comprehensive evaluation of age-editing models, we conducted assessments from two primary perspectives: age editing accuracy and identity (ID) preservation capability. As generative models become more advanced, we’ve added extra quality checks to assess: quality and visual clarity.

For Age Accuracy, the predicted age attributes of generated images were extracted using the MIVOLO pre-trained model (Kuprashevich and Tolstykh 2023), enabling quantitative measurement of alignment between edited ages and target age groups. For Identity Preservation, ID consistency was quantified by computing the cosine similarity between identity embeddings extracted from source and gen-

erated images via the AdaFace (Kim, Jain, and Liu 2022) framework, ensuring objective evaluation of facial identity retention. To thoroughly evaluate the quality of results, we used FACE++’s professional face analysis platform (Gomez-Trenado et al. 2022) for comprehensive testing. This multi-part evaluation system gives us complete performance data for our specific editing task and overall generation quality.

4.2 Comparisons with State-of-the-art Methods

Comparison methods We benchmarked our model against several state-of-the-art methods, including LATS (Or-El et al. 2020), CUSP (Gomez-Trenado et al. 2022), SAM (Alaluf, Patashnik, and Cohen-Or 2021), IpAdapter (Ye et al. 2023), PhotoMaker (Li et al. 2024) and FADING (Chen and Lathuilière 2023).

Evaluation on Quality

To evaluate the model’s performance, we first conducted extreme age editing experiments targeting 10-year-old and 80-year-old appearances.

As shown in the Figure 4, the performance of CUSP is subpar, with almost no change in facial details. LATS shows the ability to create a younger appearance but generates low-quality images with artifacts, and there is little change for aging. CUSP, IP-Adapter and PhotoMaker show almost no trend in age transformation. SAM and FADING have relatively good overall age transformation effects, but they still produce unnatural results.

We observe that most existing age editing models tend to keep facial structures largely unchanged, which is unrealistic. As shown in Figure 5, we conduct a fine-grained age comparison. We find that both SAM and FADING only make slight adjustments to the original facial structure (e.g., adding wrinkles), but this doesn’t reflect the true aging process. In contrast, our model generates results that align with the natural transition from youth to old age, with a smooth and high-quality aging process.

Evaluation on Quantity In Table 1, we evaluated the age-editing capabilities of various models across target ages ranging from 10 to 70 years, calculating the Mean Absolute

Method \ Metric	Age MAE ↓								Similarity ↑	Image Quality	
	10	20	30	40	50	60	70	Average		FaceQ ↑	Blur ↓
LATS	5.439	13.510	21.708	29.005	33.090	35.456	40.298	25.501	0.39	62.957	1.087
CUSP	23.210	4.142	4.945	6.293	6.337	<u>5.457</u>	35.120	12.215	0.55	64.429	2.015
SAM	3.959	<u>3.224</u>	4.816	<u>5.857</u>	<u>5.633</u>	6.673	<u>7.224</u>	<u>5.341</u>	0.42	66.217	1.674
IP-Adapter	22.087	12.172	10.592	13.955	20.091	28.137	36.836	20.553	<u>0.63</u>	66.337	0.768
PhotoMaker	22.126	13.983	11.668	13.405	17.531	24.502	33.288	19.500	0.30	<u>72.523</u>	<u>0.460</u>
FADING	<u>2.820</u>	3.540	<u>4.640</u>	6.420	8.260	8.400	10.280	6.337	<u>0.63</u>	60.886	1.844
Ours	1.360	2.020	3.780	5.080	4.800	4.620	5.220	3.840	0.67	74.043	0.433

Table 1: Quantitative comparison on CelebA-HQ. The best result is shown in **bold**, and the second best is underlined.

Error (MAE) for all results. A lower MAE indicates superior aging accuracy. Our analysis revealed that our model outperformed all competing methods across all age groups. Notably, our model demonstrated a significant lead in the average MAE, surpassing existing benchmarks. Our model achieved significantly highest input-output similarity than all other methods, demonstrating superior ID retention during age manipulation.

Dataset	Age MAE ↓			Face Similarity ↑		
	SAM	FADING	Ours	SAM	FADING	Ours
MORPH	4.665	4.473	3.239	0.701	0.405	0.703
AgeDB	5.667	5.011	3.542	0.690	0.385	0.696
FFHQ	5.785	4.65	3.588	0.642	0.444	0.697
CACD	4.624	4.781	2.827	0.674	0.417	0.72

Table 2: Quantitative comparison on more dataset.

In Table 2, in order to verify the robustness of the model, we also tested it on some commonly used data sets, and our age mae and face similarity were the best performers.

These results validate that our approach effectively preserves identity features while enabling robust age transformations, outperforming existing models in both identity stability and edit controllability.

4.3 Ablation Studies

Our model incorporates age-conditioned and ID-conditioned controls in the cross-attention mechanism. To assess whether these controls are decoupled, we conducted ablation studies by removing Age and ID condition control module in the multi-cross attention computation respectively during training. As shown in Figure 6 and Table 3, when only age control was applied, the generated images exhibited age progression but lacked identity preservation, maintaining only coarse attributes. Conversely, when only ID control was applied, the identity was preserved, but age changes were negligible. These results confirm that our multi-cross attention mechanism effectively decouples age and identity, allowing independent control over both attributes, a key improvement over existing methods.

For the Age Classifier Guidance (ACG) module, we further investigate its impact on age-related facial editing. When we removed the ACG module from the training

Metric \ Control	Age MAE ↓	Face Similarity ↑
full model	3.840	0.67
W/O Age	20.516	0.67
W/O ID	4.174	0.06
W/O ACG	3.915	0.67

Table 3: Ablation study on condition control pipeline, we observed an increase in Age MAE. This indicates that while the ACG module does not drastically change the overall performance, it plays a subtle but important role in guiding the model toward more accurate and realistic age transformations during training.

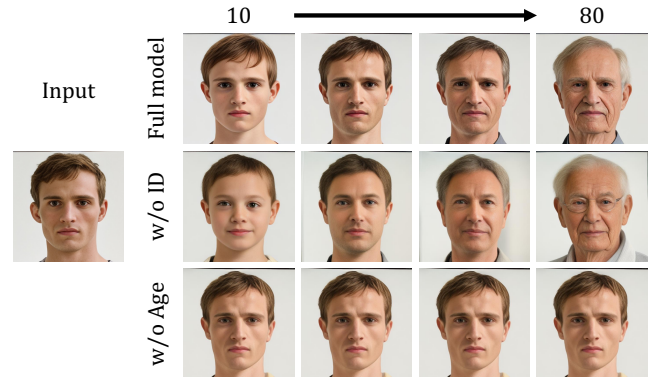


Figure 6: Ablation study on different condition control. We demonstrate the performance of TimeMachine with different condition control at ages of 10, 30, 50, and 80.

5 Conclusion

In this work, we propose a novel approach to **TimeMachine** that achieves precise age modification while preserving identity. We construct a high-quality **HFFA** (High-quality Fine-grained Facial-Age) dataset to support age-related editing tasks. Our Condition Projection Module and Decoupled Multi-Cross-Attention mechanism enable effective control over both facial appearance and aging. Additionally, we introduce the lightweight Age Classifier Guidance (ACG) module to enhance attribute supervision. Experiments demonstrate that our method outperforms state-of-the-art approaches in age accuracy and identity preservation. This work advances facial age editing with potential applications in digital aging, character design, and beyond.

References

- Alaluf, Y.; Patashnik, O.; and Cohen-Or, D. 2021. Only a matter of style: Age transformation using a style-based regression model. *ACM TOG*.
- Chen, B.-C.; Chen, C.-S.; and Hsu, W. H. 2014. Cross-age reference coding for age-invariant face recognition and retrieval. In *European conference on computer vision*, 768–783. Springer.
- Chen, X.; and Lathuilière, S. 2023. Face aging via diffusion-based editing. *arXiv preprint arXiv:2309.11321*.
- Couairon, G.; Verbeek, J.; Schwenk, H.; and Cord, M. 2022. Diffedit: Diffusion-based semantic image editing with mask guidance. *arXiv preprint arXiv:2210.11427*.
- Dhariwal, P.; and Nichol, A. 2021. Diffusion models beat gans on image synthesis. In *NeurIPS*.
- Gomez-Trenado, G.; Lathuilière, S.; Mesejo, P.; and Cordon, O. 2022. Custom structure preservation in face aging. In *ECCV*.
- Goodfellow, I. J.; Pouget-Abadie, J.; Mirza, M.; Xu, B.; Warde-Farley, D.; Ozair, S.; Courville, A.; and Bengio, Y. 2014. Generative adversarial nets. In *NeurIPS*.
- Guo, Z.; Wu, Y.; Zhuowei, C.; Zhang, P.; He, Q.; et al. 2024. Pulid: Pure and lightning id customization via contrastive alignment. In *NeurIPS*.
- Härkönen, E.; Hertzmann, A.; Lehtinen, J.; and Paris, S. 2020. Ganspace: Discovering interpretable gan controls. In *NeurIPS*.
- He, S.; Liao, W.; Yang, M. Y.; Song, Y.-Z.; Rosenhahn, B.; and Xiang, T. 2021. Disentangled lifespan face synthesis. In *ICCV*.
- Ho, J.; Jain, A.; and Abbeel, P. 2020. Denoising diffusion probabilistic models. In *NeurIPS*.
- Hsu, G.-S.; Xie, R.-C.; and Chen, Z.-T. 2021. Wasserstein Divergence GAN With Cross-Age Identity Expert and Attribute Retainer for Facial Age Transformation. *IEEE Access*.
- Karras, T.; Aila, T.; Laine, S.; and Lehtinen, J. 2017. Progressive growing of gans for improved quality, stability, and variation. *arXiv preprint arXiv:1710.10196*.
- Karras, T.; Laine, S.; and Aila, T. 2019. A style-based generator architecture for generative adversarial networks. In *CVPR*.
- Karras, T.; Laine, S.; Aittala, M.; Hellsten, J.; Lehtinen, J.; and Aila, T. 2020. Analyzing and improving the image quality of stylegan. In *CVPR*.
- Kawar, B.; Zada, S.; Lang, O.; Tov, O.; Chang, H.; Dekel, T.; Mosseri, I.; and Irani, M. 2023. Imagic: Text-based real image editing with diffusion models. In *CVPR*.
- Kim, M.; Jain, A. K.; and Liu, X. 2022. Adaface: Quality adaptive margin for face recognition. In *CVPR*.
- Kuprashevich, M.; and Tolstykh, I. 2023. Mivolo: Multi-input transformer for age and gender estimation. In *International Conference on Analysis of Images, Social Networks and Texts*.
- Li, J.; Li, D.; Xiong, C.; and Hoi, S. 2022. Blip: Bootstrapping language-image pre-training for unified vision-language understanding and generation. In *ICML*.
- Li, Z.; Cao, M.; Wang, X.; Qi, Z.; Cheng, M.-M.; and Shan, Y. 2024. Photomaker: Customizing realistic human photos via stacked id embedding. In *CVPR*.
- Liu, L.; Ren, Y.; Lin, Z.; and Zhao, Z. 2022. Pseudo numerical methods for diffusion models on manifolds. *arXiv preprint arXiv:2202.09778*.
- Liu, Y.; Li, Q.; and Sun, Z. 2019. Attribute-Aware Face Aging With Wavelet-Based Generative Adversarial Networks. In *CVPR*.
- Matuzevičius, D. 2024. Diverse Dataset for Eyeglasses Detection: Extending the Flickr-Faces-HQ (FFHQ) Dataset. *Sensors*.
- Moschoglou, S.; Papaioannou, A.; Sagonas, C.; Deng, J.; Kotsia, I.; and Zafeiriou, S. 2017. AgeDB: The First Manually Collected, In-the-Wild Age Database. In *2017 IEEE Conference on Computer Vision and Pattern Recognition Workshops (CVPRW)*, 1997–2005.
- Or-El, R.; Sengupta, S.; Fried, O.; Shechtman, E.; and Kemelmacher-Shlizerman, I. 2020. Lifespan age transformation synthesis. In *ECCV*.
- Panis, G.; Lanitis, A.; Tsapatsoulis, N.; and Cootes, T. F. 2016. Overview of research on facial ageing using the FG-NET ageing database. *Iet Biometrics*.
- Radford, A.; Kim, J. W.; Hallacy, C.; Ramesh, A.; Goh, G.; Agarwal, S.; Sastry, G.; Askell, A.; Mishkin, P.; Clark, J.; et al. 2021. Learning transferable visual models from natural language supervision. In *ICML*.
- Ricanek, K.; and Tesafaye, T. 2006. Morph: A longitudinal image database of normal adult age-progression. In *7th international conference on automatic face and gesture recognition (FGR06)*.
- Rombach, R.; Blattmann, A.; Lorenz, D.; Esser, P.; and Ommer, B. 2022. High-resolution image synthesis with latent diffusion models. In *CVPR*.
- Saharia, C.; Chan, W.; Saxena, S.; Li, L.; Whang, J.; Denton, E. L.; Ghasemipour, K.; Gontijo Lopes, R.; Karagol Ayan, B.; Salimans, T.; et al. 2022. Photorealistic text-to-image diffusion models with deep language understanding. In *Advances in neural information processing systems*.
- Shen, Y.; Gu, J.; Tang, X.; and Zhou, B. 2020. Interpreting the latent space of gans for semantic face editing. In *CVPR*.
- Tang, R.; Liu, L.; Pandey, A.; Jiang, Z.; Yang, G.; Kumar, K.; Stenatorp, P.; Lin, J.; and Ture, F. 2022. What the daam: Interpreting stable diffusion using cross attention. *arXiv preprint arXiv:2210.04885*.
- Team, Q. 2025. Qwen2.5-VL.
- Tov, O.; Alaluf, Y.; Nitzan, Y.; Patashnik, O.; and Cohen-Or, D. 2021. Designing an encoder for stylegan image manipulation. *ACM TOG*.
- Wang, Q.; Bai, X.; Wang, H.; Qin, Z.; Chen, A.; Li, H.; Tang, X.; and Hu, Y. 2024. Instantid: Zero-shot identity-preserving generation in seconds. *arXiv preprint arXiv:2401.07519*.

Yang, H.; Huang, D.; Wang, Y.; and Jain, A. K. 2019. Learning continuous face age progression: A pyramid of GANs. *IEEE TPAMI*.

Yao, X.; Puy, G.; Newson, A.; Gousseau, Y.; and Hellier, P. 2021. High resolution face age editing. In *ICPR*.

Ye, H.; Zhang, J.; Liu, S.; Han, X.; and Yang, W. 2023. Ip-adapter: Text compatible image prompt adapter for text-to-image diffusion models. *arXiv preprint arXiv:2308.06721*.

Zheng, Y.; Yang, H.; Zhang, T.; Bao, J.; Chen, D.; Huang, Y.; Yuan, L.; Chen, D.; Zeng, M.; and Wen, F. 2022. General facial representation learning in a visual-linguistic manner. In *CVPR*.

Zhou, S.; Chan, K.; Li, C.; and Loy, C. C. 2022. Towards robust blind face restoration with codebook lookup transformer. In *Advances in Neural Information Processing Systems*.

Supplementary Materials for

TimeMachine: Fine-Grained Facial Age Editing with Identity Preservation

Our supplementary material provides additional details about our method and experimental results, summarized as follows:

In Section A, we provide an in-depth analysis of the **HFFA** to better understand its unique features and advantages. This section covers the following:

- **Image preprocessing** in Section A.1: we discuss the preprocessing steps applied to the images in the dataset, which include cropping, resizing, and enhancing image quality to ensure consistency in age-related tasks.
- **Comparison with other age datasets** in Section A.2: we compare HFFA with other prominent facial age datasets. Key differences such as image resolution, age distribution, and annotation accuracy are highlighted, emphasizing the strengths of HFFA in supporting high-precision age estimation and age manipulation tasks.
- **Analysis of the age codebook** in Section A.3: we provide an analysis of the age codebook, which is an essential component for age editing in HFFA.

In Section B, we present additional experiments and results on **TimeMachine**, a model designed for age manipulation. The following experiments are detailed in this section::

- **Condition control analysis** in Section B.1: we conduct a detailed investigation into how varying the age scale parameter influences the visual outcomes of age editing.
- **Decoupled attributes in Multi-CA** in Section B.2: we visualize the attention maps to show that the identity and age branches focus on different facial features, demonstrating the decoupling ability of Multi-CA in handling age and identity separately.
- **Other attribute edits by Multi-CA** in Section B.3: we provide experiments on gender editing, demonstrating the robustness of Multi-Cross Attention (Multi-CA) in handling various attribute manipulations.
- **Plug-and-play results** in Section B.4: we provide the plug-and-play design of TimeMachine, which requires no retraining or fine-tuning.
- **User study** result in Section B.5: we present the outcomes of a comprehensive user study, in which participants consistently favored our results over competing methods.
- **More qualitative results** in Section B.6: we provide additional age editing results, highlighting the impressive performance of our model.

A More Details of HFFA

A.1 Details of Image Preprocessing

To obtain a high-quality facial image training dataset, we first perform dataset filtering. We select images with a single person, where the face occupies more than 5% of the image area. The face region is cropped, followed by super-resolution (SR) quality enhancement on the cropped area. As shown in the Figure 7, the preprocessed images exhibit a significant improvement in quality compared to the original ones.



Figure 7: Results of the preprocessing steps, including cropping and super-resolution (SR) enhancement.

In the training process of Stable Diffusion (SD), the caption of the input image is also crucial. We use the Qwen2.5-VL72BInstruct model (Team 2025) for image captioning. As shown in the Figure 8, high-quality captions are generated by feeding the image and a related question into the Qwen model, resulting in precise and contextually accurate annotations. In comparison, captions generated by the widely used BLIP model (Li et al. 2022) often suffer from semantic inaccuracies, fail to capture important details, and may even misinterpret the image content, leading to lower-quality training data.

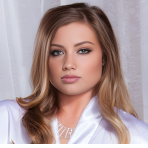


input	Qwen Question	Qwen Caption	Blip Caption
	Please provide a concise description of the image, focusing on the following aspects: Basic information: gender, age group, etc. Facial Features: Describe the person's face (e.g., eyes, nose, lips, and overall structure). Expression: What is the person's facial expression (e.g., smiling, serious, etc.)? Clothing: What is the person wearing? Describe the style and color of the outfit.	A young female, likely in her early twenties, with long wavy blonde hair, prominent brown eyes, a straight nose, full lips, and an oval face structure, has a serious expression while wearing a white satin robe over a sheer top with a silver necklace, with a confident posture and neutral body language, against a plain white background.	a woman in a white robe posing for a picture
	Posture and Actions: Posture: Is the person standing or sitting? How is their posture (e.g., confident, relaxed)? Body Language: What is the person's body language? Are they holding anything or making any gestures?	A young child, likely a toddler of indeterminate gender, has round cheeks, dark eyes, a small nose, and full lips, and is smiling joyfully while wearing a white and black plush panda hat; the child is shirtless, sitting with a relaxed posture, and appears to be reaching out with both hands, conveying a sense of playful engagement.	a baby wearing a sheep hat
		The male, likely in his middle age group, has a round face with prominent eyes, a straight nose, full lips, and a mustache, wears a dark-colored suit jacket over a black shirt, accessorized with an earring, sits with a relaxed yet confident posture, and has a slight smile on his face, all while being captured against a blurred background of bookshelves.	a man with a mustache

Figure 8: Overview of the captioning process for our dataset. We use the Qwen model to generate captions by asking specific questions about the images, and then use the obtained responses as the captions. The results are compared with those generated by the BLIP model.

A.2 Comparison with other Age Datasets

In order to highlight the strengths and unique advantages of our dataset, we conducted a comparison with several commonly used age-related facial datasets, such as MORPH (Ricanek and Tesafaye 2006), AGEDB (Moschoglou et al. 2017), FFHQ (Karras, Laine, and Aila 2019), and CACD (Chen, Chen, and Hsu 2014). This comparison helps contextualize the features of our HFFA dataset in terms of key aspects like resolution, size, and age range.

Dataset	Resolution	Size	Age Range
HFFA	1024*1024	1M+	1-85
MORPH	180*180	5W+	0-60
AgeDB	Variable	16W+	1-101
CACD	250*250	16W+	14-62
FFHQ-Aging	1024*1024	7W	0-70+

Table 4: Comparison of different Age-datasets

As shown in Table 4, HFFA stands out notably in terms of image resolution. All images in the HFFA dataset are provided in high-resolution (1024×1024), ensuring that facial details are captured with exceptional clarity. In contrast, other datasets such as MORPH and CACD feature much lower resolutions, with sizes of 180×180 and 250×250 respectively. This difference in resolution gives HFFA a clear advantage when it comes to capturing fine details such as skin texture, wrinkles, and subtle facial expressions, which are crucial for high-quality facial age editing and related tasks. Additionally, although FFHQ-Aging also offers images at a resolution of 1024×1024, it is limited by a smaller sample size (7W) and the absence of detailed image cap-

tions, making it less suitable for fine-grained facial age editing compared to HFFA.

Dataset	Gender Caption	Multi-age per ID	Semantic Map	Face kps Face bbox	Face embedding	Age embedding	Image Caption
MORPH	✓	✗	✗	✗	✗	✗	✗
AgeDB	✓	✓	✗	✗	✗	✗	✗
CACD	✓	✓	✗	✗	✗	✗	✗
FFHQ	✓	✗	✓	✗	✗	✗	✗
HFFA	✓	✗	✓	✓	✓	✓	✓
				✓ w/ the Attribute	✗ w/o. the Attribute		

Figure 9: More comparison of different Age-datasets

Furthermore, as shown in Figure 9, HFFA includes not only high-resolution images but also provides rich face-related information such as detailed image captions, face embeddings, and age embeddings. These supplementary annotations make HFFA especially valuable for training models in Stable Diffusion (SD) and other advanced generative tasks. Other datasets, on the other hand, generally lack these precise annotations, limiting their applicability for tasks that require detailed understanding of age progression and facial characteristics.

Overall, the HFFA dataset clearly outperforms in terms of resolution, data richness, and applicability, making it particularly well-suited for high-precision facial age editing and age prediction tasks. Its comprehensive annotations and superior image quality position it as an ideal choice for researchers and practitioners working on fine-grained age-related facial recognition tasks.

A.3 Pure Age embeddings in Age codebook

A critical component in the HFFA dataset is the construction of the **age codebook**. This codebook is generated by averaging all age embeddings corresponding to each specific age, with the objective of obtaining pure age-specific representations.

To ensure the age codebook remains unbiased, we validated that the averaging process does not introduce race-related bias. We constructed race-specific age codebooks by dividing the dataset into subsets based on race, then computed the cosine similarity between each race-specific codebook and the overall codebook. This step confirms that the age codebook accurately reflects age characteristics without being influenced by racial attributes.

Race	White	Black	Asian	Indian
Similarity \uparrow	0.998	0.976	0.994	0.989

Table 5: Similarity of race-specific age codebook

As demonstrated in Table 5, all race-specific age codebooks exhibit exceptionally high cosine similarity values (greater than 97%) with the overall age codebook. These high similarity scores confirm that the age codebook accurately captures age-specific information without being influenced by racial attributes. This validation reinforces the reliability and fairness of the HFFA dataset for age-related tasks, ensuring that the age representations are unbiased and representative across different demographic groups.

B More Experiment on TimeMachine

B.1 Analysis of Condition Control

Through comprehensive experimental analysis, we demonstrate that adjusting the age scale parameter within the multi-cross attention module during the inference phase of TimeMachine provides precise control over the intensity of age-related features in synthesized images. As shown in Figure 10, progressively increasing the age scale results in more pronounced facial wrinkles, gradual graying of hair, and other subtle age-related changes.

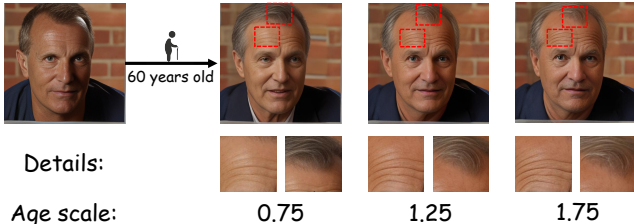


Figure 10: Visualization of age condition control by age scale

This empirical evidence underscores the effectiveness of our approach, where the multi-cross attention mechanism successfully disentangles age-related features from identity traits through training. By utilizing the age-conditioned

cross-attention layers, our model achieves highly controllable and fine-grained age editing, enabling realistic and age-appropriate transformations while preserving the integrity of the individual’s unique identity.

B.2 Decoupled Attribute in Multi-CA

In our Multi-Cross-Attention (Multi-CA) module, we decouple condition hidden states (text, identity, age) and compute separate cross-attention operations for each condition. This architecture is explicitly designed to achieve full disentanglement of distinct condition.

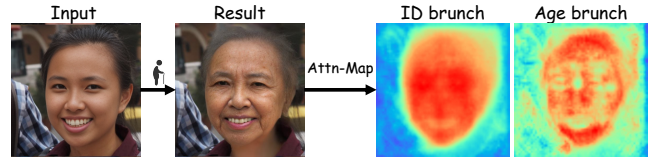


Figure 11: Visualization of attention map

To validate that the injected identity and age information are effectively isolated, we visualize the cross-attention maps in Figure 11. The analysis reveals important insights about how the model processes identity and age-related features:

Identity Branch: The attention maps consistently focus on global facial structures, such as face shape, which are critical to an individual’s unique identity. These features remain largely unaffected by age changes, indicating that the identity branch successfully preserves core identity information without being influenced by aging.

Age Branch: In contrast, the attention maps in the age branch selectively highlight local regions where aging is most visually pronounced, such as forehead wrinkles, cheek volume. These areas are particularly sensitive to age-related changes, and the attention mechanism is able to focus on them without interference from other identity features.

The cross-attention maps provide strong empirical evidence of the complete disentanglement of identity and age information within our multi-cross attention (Multi-CA) module. Identity features are captured in a holistic manner, while age features are localized to specific facial regions, ensuring that there is no mutual interference between the two types of information. This validation underscores the effectiveness of our approach in isolating and manipulating age-related features while preserving individual identity characteristics.

B.3 Other Attribute edit by Multi-CA

To validate the generalizability of Multi-Cross-Attention (Multi-CA) in attribute editing, we also tested it on other attributes. Here, we demonstrate its versatility using gender editing as an example.

For the training data, we extracted gender information and gender embeddings using the MIVOLO model (Kuprashevich and Tolstykh 2023), consistent with the method described in the main text, and then constructed the codebook.

As shown in the Figure 12, the model works effectively for gender editing, producing high-quality and natural edits.

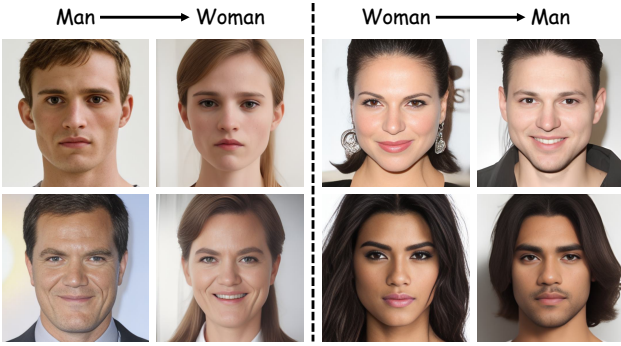


Figure 12: Gender editing result by Multi-CA

The generated images exhibit strong fidelity to the original input, with subtle yet accurate gender transformations.

We also conducted some quantitative tests on gender editing. We randomly selected 100 images from the CelebA-HQ dataset (Karras et al. 2017) and performed gender editing on them. The accuracy of the editing and the face similarity post-editing were evaluated. As shown in the Table 6, the model achieved high editing accuracy and strong face similarity, demonstrating the effectiveness of the approach.

Task	Gender Accuracy \uparrow	Face Similarity \uparrow
male \rightarrow female	98%	0.680
female \rightarrow male	96%	0.679

Table 6: Quantitative result on gender editing

These results are promising and demonstrate the generalizability of Multi-CA in performing attribute editing across diverse domains.

B.4 Plug-and-Play Design

Our model is trained on the SD1.5 base model, with modifications limited to the cross-attention layers and supplementary projection modules. To evaluate the portability of our framework, in Figure 13, we conducted tests without retraining the model, instead replacing the base model with alternatives such as Realistic_Vision_V4.0^{*} and dreamshaper-8[†]. Remarkably, our model seamlessly adapts to these diverse base architectures, maintaining robust performance in age-editing accuracy and identity (ID) preservation across all configurations. This demonstrates the plug-and-play compatibility of our approach, enabling flexible integration with varied generative backbones while preserving core functionality.

B.5 User Study

To evaluate the perceptual quality of our results, we conducted a user study comparing our method with two baselines: SAM (Alaluf, Patashnik, and Cohen-Or 2021) and

^{*}https://huggingface.co/SG161222/Realistic_Vision_V4.0_noVAE

[†]<https://huggingface.co/Lykon/dreamshaper8>

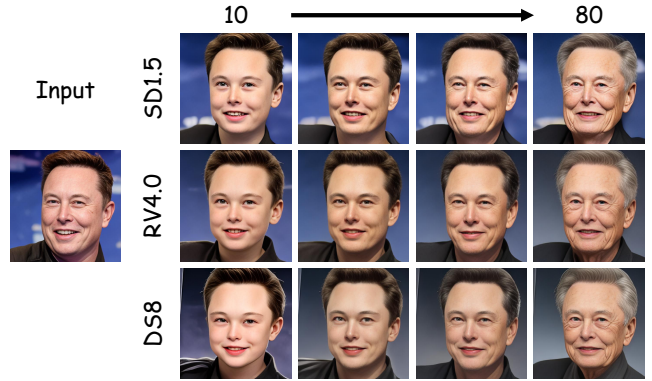


Figure 13: Plug-and-play property of TimeMachine, compatible with different base models. We demonstrate the performance of TimeMachine with different base models at ages of 10, 30, 50, and 80.

FADING (Chen and Lathuilière 2023). A total of 25 participants were shown side-by-side comparisons of facial age editing results generated by our method and the baseline models. For each pair, participants were asked to choose the image they found more visually realistic and identity-preserving.

Method	Ours vs. SAM	Ours vs. FADING
User Preference	73.87%	85.07%

Table 7: User Study on different Models

As shown in Table 7, our method was preferred over SAM (Alaluf, Patashnik, and Cohen-Or 2021) in 73.87% of cases and over FADING (Chen and Lathuilière 2023) in 85.07% of cases, demonstrating a clear user preference for the quality and consistency of our age editing results.

B.6 More Qualitative Results

In Figure 14, comparative qualitative results demonstrate that our method achieves superior performance in the generation of high-quality fine-grained age-specific images compared to the SAM (Alaluf, Patashnik, and Cohen-Or 2021) and FADING (Chen and Lathuilière 2023) approaches. In particular, our framework successfully avoids common artifacts, such as structural collapse of facial features and implausible partial modifications that compromise facial authenticity. The proposed system effectively preserves the intrinsic identity information from source images while adaptively integrating age-specific characteristics learned by our TimeMachine. This synergistic combination enables the generation of high-fidelity facial images that maintain both identity consistency and age-appropriate morphological features.



Figure 14: More qualitative results. Our method achieves significant improvements in both structural preservation and age transformation accuracy compared to existing methods.